Inorganic Chemistry

Article

pubs.acs.org/IC

Syntheses, Structures, Optical and Magnetic Properties of $Ba_2ML\!nSe_5$ (M = Ga, In; *Ln* = Y, Nd, Sm, Gd, Dy, Er)

Wenlong Yin,[†,‡,§] Kai Feng,[†,‡,§] Wendong Wang,[∥] Youguo Shi,[⊥] Wenyu Hao,[†,‡,§] Jiyong Yao,*[,†,‡] and Yicheng Wu[†,‡]

[†]Center for Crystal Research and Development and [‡]Key Laboratory of Functional Crystals and Laser Technology, Technical Institute of Physics and Chemistry, Chinese Academy of Sciences, Beijing 100190, P.R. China

[§]Graduate University of the Chinese Academy of Sciences, Beijing 100049, China

[∥]School of Science, Beijing University of Post and Telecommunication, Beijing 100876, China

[⊥]Beijing National Laboratory for Condensed Matter Physics, Institute of Physics, Chinese Academy of Sciences, Beijing 100190, China

Supporting Information

ABSTRACT: The twelve quaternary rare-earth selenides $Ba_2ML\!nSe_5$ (M = Ga, In; *Ln* = Y, Nd, Sm, Gd, Dy, Er) have been synthesized for the first time. The compounds $Ba_2GaL\!nSe_5$ (*Ln* = Y, Nd, Sm, Gd, Dy, Er) are isostructural and crystallize in a new structure type in the centrosymmetric space group $P\bar{1}$ of the triclinic system while the isostructural compounds $Ba_2InL\!nSe_5$ (*Ln* = Y, Nd, Sm, Gd, Dy, Er) belong to the Ba_2BiInS_5 structure type and crystallize in the noncentrosymmetric space group $Cmc2_1$ of the orthorhombic system. The structures contain infinite one-dimensional anionic chains $^{\infty}_{1}[GaL\!nSe_5]^{4-}$ and $^{\infty}_{1}[InL\!nSe_5]^{4-}$, and both chains are built from $L\!nSe_6$ octahedra and MSe_4 (M = Ga, In) tetrahedra in the corresponding selenides. As deduced from the diffuse reflectance spectra, the band gaps of most $Ba_2ML\!nSe_5$ (M = Ga, In; *Ln* = Y, Nd, Sm, Gd, Dy, Er) compounds are around 2.2 eV. The magnetic susceptibility measurements on $Ba_2GaGdSe_5$ and $Ba_2InL\!nSe_5$ (Ln = Nd, Gd, Dy, Er) indicate that they are paramagnetic and obey the Curie–Weiss law, while the magnetic susceptibility of $Ba_2InSmSe_5$ deviates from the Curie–Weiss law as a result of the crystal field splitting. Furthermore, Ba_2InYSe_5 exhibits a strong second harmonic generation response close to that of $AgGaSe_2$, when probed with the 2090 nm laser as fundamental wavelength.

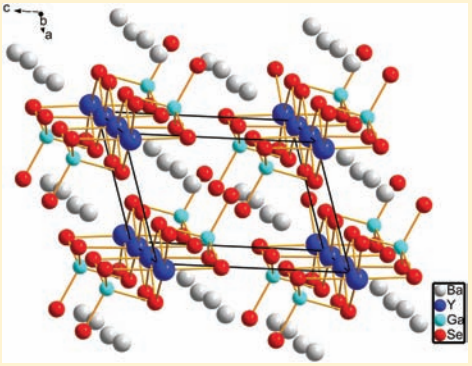

INTRODUCTION

Rare-earth elements (*Ln*) are of fundamental interest because of the diversity in the geometry of the *Ln*-centered coordination polyhedra and the connectivity between them, the lanthanide contraction, and the magnetic and optical properties related to the 4f electrons.[1,2] In recent years, extensive research has been done on the synthesis and characterization of rare-earth chalcogenides, which led to the discovery of many new multinary rare-earth chalcogenides with rich structures and interesting magnetic, electronic, luminescent, thermoelectric, and nonlinear optical properties.[3−31] Most of these rare-earth chalcogenides also contain a d-block transition metal. For example, $KCuCe_2S_6$ possesses the disulfide S_2^{2-} anions;[3] $K_2Cu_2CeS_4$ and $CsCuCeS_3$ exhibit valence fluctuations with the unusual formal valence representations $(K^+)_2(Cu^+)_2Ce^{3+}(S^{2-})_3(S^-)$ and $Cs^+Ce^{3+}Cu^+(S^{2-})_2(S^-)$;[3,4] $AYbMQ_3$ (A = Rb, Cs; M = Zn, Mn; Q = S, Se) show broad magnetic transitions at ≈10 K;[5] $EuLnCuS_3$ (Ln = Y, Gd–Lu) display ferromagnetic or ferrimagnetic transitions at low temperatures;[6] $AL\!nMQ_3$ (A = Rb, Cs; *Ln* = rare-earth metal; M = Mn, Co, Zn, Cd, Hg; Q = S, Se, Te) are magnetic semiconductors offering flexibility in band gap engineering by controlling the composition and crystal orientation;[26−30] and $Cs_xLn_2Cu_{6-x}Te_6$ (*Ln* = La, Ce, Pr) exhibit some interesting thermoelectric properties.[31]

Compared with the extensive research on rare-earth chalcogenides containing a d-block metal, the research on rare-earth chalcogenides containing a main-group p-block element is relatively scarce. However, chalcogenides with a combination of f-block and p-block elements were also found to exhibit unusual structures and physical properties. For example, the $ZnY_6Si_2S_{14}$,[19] $La_2Ga_2GeS_8$,[20] $Eu_2Ga_2GeS_7$,[20] La_4InSbS_9,[21] and Sm_4GaSbS_9,[22] compounds, especially the latter three, were reported to exhibit strong second harmonic generation (SHG) responses in middle IR. In this study, we focus on the quaternary A/M/*Ln*/Q (A = alkaline-earth metal; M = group IIIA metal Ga, In; *Ln* = rare-earth; Q = S, Se, Te) system. The MQ_4 (M = In, Ga; Q = S, Se) tetrahedra are the fundamental structural units in many IR nonlinear optical (NLO)

Received: March 22, 2012
Published: June 6, 2012

   dx.doi.org/10.1021/ic300604a | *Inorg. Chem.* 2012, 51, 6860–6867

Table 1. Crystal Data and Structure Refinements for $Ba_2GaLnSe_5$ (*Ln* = Y, Nd, Sm, Gd, Dy, Er)[a]

	Ba_2GaYSe_5	$Ba_2GaNdSe_5$	$Ba_2GaSmSe_5$	$Ba_2GaGdSe_5$	$Ba_2GaDySe_5$	$Ba_2GaErSe_5$
fw	828.11	883.44	889.55	896.45	901.70	906.46
a (Å)	7.288(2)	7.290(2)	7.3017(2)	7.283(2)	7.277(2)	7.272(2)
b (Å)	8.660(2)	8.791(2)	8.7635(3)	8.706(2)	8.654(2)	8.626(2)
c (Å)	9.388(2)	9.470(2)	9.4554(3)	9.408(2)	9.379(2)	9.362(2)
α (deg)	103.51(3)	103.77(3)	103.672(1)	103.65(3)	103.53(3)	103.41(3)
β (deg)	103.04(3)	102.91(3)	102.963(2)	103.02(3)	103.07(3)	103.13(3)
γ (deg)	107.43(3)	107.72(3)	107.637(1)	107.52(3)	107.43(3)	107.39(3)
V (Å^3)	520.9(2)	532.0(2)	530.88(3)	523.8(2)	519.3(2)	516.6(2)
ρ_c (g/cm3)	5.279	5.515	5.565	5.684	5.767	5.828
μ (cm^{-1})	32.922	31.634	32.343	33.506	34.607	35.678
$R(F)^b$	0.0382	0.0318	0.0237	0.0350	0.0418	0.0387
$R_W(F_o^2)^c$	0.0768	0.0670	0.0627	0.0777	0.0999	0.0847

[a]For all structures, Z = 2, space group = $P\bar{1}$, T = 153 (2) K, and λ = 0.71073 Å. [b]$R(F) = \sum||F_o| - |F_c||/\sum|F_o|$ for $F_o^2 > 2\sigma(F_o^2)$. [c]$R_w(F_o^2) = \{\sum[w(F_o^2 - F_c^2)^2]/\sum wF_o^4\}^{1/2}$ for all data; $w^{-1} = \sigma^2(F_o^2) + (z\,P)^2$, where $P = (\mathrm{Max}(F_o^2, 0) + 2\,F_c^2)/3$.

Table 2. Crystal Data and Structure Refinements for $Ba_2InLnSe_5$ (*Ln* = Y, Nd, Sm, Gd, Dy, Er)[a]

	Ba_2InYSe_5	$Ba_2InNdSe_5$	$Ba_2InSmSe_5$	$Ba_2InGdSe_5$	$Ba_2DyInSe_5$	$Ba_2InErSe_5$
fw	873.21	928.54	934.65	941.55	946.80	951.56
a (Å)	4.2519(9)	4.2980(9)	4.2868(9)	4.2695(9)	4.2529(9)	4.2345(8)
b (Å)	18.740(4)	18.807(4)	18.805(4)	18.790(4)	18.726(4)	18.723(4)
c (Å)	13.271(3)	13.227(3)	13.250(3)	13.269(3)	13.258(3)	13.255(3)
V (Å^3)	1057.4(4)	1069.2(4)	1068.1(4)	1064.5(4)	1055.8(4)	1050.9(4)
Flack parameter	0.01(1)	0.04(2)	0.02(2)	0.06(2)	0.03(2)	0.04(2)
ρ_c (g/cm3)	5.485	5.768	5.812	5.875	5.956	6.014
μ (cm^{-1})	32.070	31.119	31.786	32.608	33.672	34.705
$R(F)^b$	0.0211	0.0324	0.0264	0.0309	0.0251	0.0375
$R_W(F_o^2)^c$	0.0417	0.0699	0.0628	0.0655	0.0586	0.0824

[a]For all structures, Z = 4, space group = $Cmc2_1$, T = 153 (2) K, and λ = 0.71073 Å. [b]$R(F) = \sum||F_o| - |F_c||/\sum|F_o|$ for $F_o^2 > 2\sigma(F_o^2)$. [c]$R_w(F_o^2) = \{\sum[w(F_o^2 - F_c^2)^2]/\sum wF_o^4\}^{1/2}$ for all data; $w^{-1} = \sigma^2(F_o^2) + (z\,P)^2$, where $P = (\mathrm{Max}(F_o^2, 0) + 2\,F_c^2)/3$.

chalcogenides.[32−40] The interplay of the covalent M−Q bonding with the ionic *Ln*−Q or A−Q bonding and the combination of these MQ_4 units with magnetic rare-earth cations in one chalcogenide may generate multifunctional materials with intriguing structures. The incorporation of an alkaline-earth metal in this system may have the additional advantage of enlarging the band gap, which may help to increase the laser damage threshold once a NLO material is found. So far, only two series of calcium chalcogenides, the $Ca_4In_4Ln_2Q_{13}$ (*Ln* = La, Nd, Sm, Gd; Q = S, Se)[23] and $CaInYbQ_4$ (Q = S, Se) compounds,[24] were reported in this system about twenty years ago. Our systematic exploratory efforts have led to the discovery of 12 new members in this family, namely, the Ba_2MLnSe_5 (M = Ga, In; *Ln* = Y, Nd, Sm, Gd, Dy, Er) selenides. Interestingly, they exhibit two different structure types: the six Ga selenides $Ba_2GaLnSe_5$ (*Ln* = Y, Nd, Sm, Gd, Dy, Er) are isostructural and crystallize in a new structure type in the centrosymmetric space group $P\bar{1}$ of the triclinic system, while the isostructural $Ba_2InLnSe_5$ (*Ln* = Y, Nd, Sm, Gd, Dy, Er) compounds crystallize in the noncentrosymmetric space group $Cmc2_1$ of the orthorhombic system. In this paper, we detail the synthesis, structural characterization, linear and nonlinear optical properties, and magnetic properties of Ba_2MLnSe_5 (M = Ga, In; *Ln* = Y, Nd, Sm, Gd, Dy, Er).

EXPERIMENTAL SECTION

Syntheses. Ba was purchased from Aladdin Co., Ltd. with the purity of 99%. Ga, In, and Se were purchased from Sinopharm Chemical Reagent Co., Ltd. with the purities of 4N. *Ln* (*Ln* = Y, Nd, Sm, Gd, Dy, Er) were purchased from Alfa Aesar China (Tianjin) Co., Ltd. with the purity of 3N. All of the above chemicals were used without further purification. The binary starting materials, BaSe, Ga_2Se_3, and In_2Se_3 were prepared from the direct reactions of the elements at high temperatures in sealed silica tubes evacuated to 10^{-3} Pa.

$Ba_2GaLnSe_5$ (*Ln* = Y, Nd, Sm, Gd, Dy, Er). The mixtures of BaSe (0.433 g, 2 mmol), Ga_2Se_3 (0.188 g, 0.5 mmol), *Ln* (*Ln* = Y, Nd, Sm, Gd, Dy, Er, 1 mmol), and Se (0.118 g, 1.5 mmol) were ground and loaded into 12 mm inner-diameter fused-silica tubes under an Ar atmosphere in a glovebox, then flame-sealed under a high vacuum of 10^{-3} Pa. The tubes were then placed in computer-controlled furnaces and heated to 1373 K in 24 h, left for 48 h, cooled to 593 K at a rate of 3 K/h, and finally cooled to room temperature by switching off the furnace. Block-shaped crystals with the color of yellow were found in the ampules. The crystals are stable in air.

$Ba_2InLnSe_5$ (*Ln* = Y, Nd, Sm, Gd, Dy, Er). The mixtures of BaSe (0.433 g, 2 mmol), In_2Se_3 (0.233 g, 0.5 mmol), *Ln* (*Ln* = Y, Nd, Sm, Gd, Dy, Er, 1 mmol), and Se (0.118 g, 1.5 mmol) were ground and loaded into fused-silica tubes under an Ar atmosphere in a glovebox, then flame-sealed under a high vacuum of 10^{-3} Pa. The tubes were then placed in computer-controlled furnaces and heated to 1323 K in 20 h, left for 48 h, cooled to 593 K at a rate of 2 K/h, and finally cooled to room temperature by switching off the furnace. Block-shaped crystals with the color of red were found in the ampules. The crystals are stable in air.

The block-shaped crystals were manually selected for structure characterization and determined as Ba_2MLnSe_5 (M = Ga, In; *Ln* = Y, Nd, Sm, Gd, Dy, Er). Analyses of the crystals with an EDX-equipped Hitachi S-4800 SEM showed the presence of Ba, M (M = Ga, In), *Ln*, and Se in the approximate ratio of 2:1:1:5.

Polycrystalline samples of Ba_2MLnSe_5 (M = Ga, In; *Ln* = Y, Nd, Sm, Gd, Dy, Er) were synthesized by solid-state reaction techniques. The mixtures of BaSe, M_2Se_3 (M = Ga, In), *Ln* (*Ln* = Y, Nd, Sm, Gd, Dy,

dx.doi.org/10.1021/ic300604a | Inorg. Chem. 2012, 51, 6860−6867

Table 3. Selected Interatomic Distances (Å) for $Ba_2GaLnSe_5$ (*Ln* = Y, Nd, Sm, Gd, Dy, Er)

	Ba_2GaYSe_5	$Ba_2GaNdSe_5$	$Ba_2GaSmSe_5$	$Ba_2GaGdSe_5$	$Ba_2GaDySe_5$	$Ba_2GaErSe_5$
Ba1−Se5	3.224(1)	3.235(1)	3.2339(6)	3.230(1)	3.222(1)	3.218(1)
Ba1−Se5	3.271(1)	3.289(1)	3.2904(5)	3.275(1)	3.269(1)	3.267(1)
Ba1−Se1	3.290(2)	3.275(2)	3.2870(6)	3.282(2)	3.287(2)	3.288(2)
Ba1−Se2	3.295(1)	3.294(1)	3.3010(6)	3.293(1)	3.292(1)	3.294(1)
Ba1−Se4	3.363(2)	3.369(2)	3.3716(6)	3.362(2)	3.356(2)	3.358(2)
Ba1−Se3	3.400(1)	3.401(1)	3.4031(6)	3.394(1)	3.388(1)	3.388(1)
Ba1−Se3	3.509(1)	3.608(1)	3.5800(7)	3.539(1)	3.506(1)	3.487(1)
Ba1−Se2	3.673(2)	3.611(2)	3.6451(7)	3.641(2)	3.667(2)	3.679(2)
Ba2−Se5	3.245(1)	3.258(1)	3.2600(5)	3.248(1)	3.241(1)	3.240(1)
Ba2−Se5	3.280(1)	3.304(1)	3.3025(6)	3.287(1)	3.278(1)	3.273(1)
Ba2−Se4	3.298(1)	3.323(1)	3.3184(7)	3.304(1)	3.294(1)	3.289(1)
Ba2−Se2	3.331(2)	3.358(2)	3.3560(6)	3.339(2)	3.330(2)	3.321(2)
Ba2−Se1	3.338(1)	3.364(1)	3.3617(6)	3.343(1)	3.338(1)	3.330(1)
Ba2−Se3	3.467(2)	3.458(2)	3.4695(6)	3.461(2)	3.458(2)	3.463(2)
Ba2−Se4	3.500(2)	3.532(1)	3.5341(6)	3.511(1)	3.495(2)	3.490(1)
Ba2−Se1	3.579(2)	3.517(2)	3.5452(7)	3.546(2)	3.574(2)	3.587(2)
Ln-Se4	2.800(2)	2.869(1)	2.8460(6)	2.824(1)	2.799(2)	2.781(1)
Ln-Se4	2.811(1)	2.878(1)	2.8540(5)	2.833(1)	2.808(1)	2.790(1)
Ln-Se2	2.852(1)	2.923(1)	2.9001(6)	2.879(1)	2.850(1)	2.836(1)
Ln-Se1	2.859(1)	2.937(0)	2.9115(6)	2.887(1)	2.859(1)	2.839(1)
Ln-Se3	2.988(1)	3.038(1)	3.0259(5)	3.007(1)	2.989(1)	2.975(1)
Ln-Se3	3.012(2)	3.063(2)	3.0497(6)	3.031(2)	3.010 (2)	2.996(2)
Ga−Se5	2.353(2)	2.347(2)	2.3501(7)	2.347(2)	2.349(2)	2.346(2)
Ga−Se2	2.398(2)	2.403(1)	2.4018(7)	2.401(1)	2.396(1)	2.396(1)
Ga−Se1	2.397(1)	2.404(1)	2.4030(7)	2.400(1)	2.395(1)	2.395(1)
Ga−Se3	2.481(1)	2.484(1)	2.4837(8)	2.479(1)	2.475(1)	2.477(1)

Table 4. Selected Interatomic Distances (Å) for $Ba_2InLnSe_5$ (*Ln* = Y, Nd, Sm, Gd, Dy, Er)

	Ba_2InYSe_5	$Ba_2InNdSe_5$	$Ba_2InSmSe_5$	$Ba_2InGdSe_5$	$Ba_2InDySe_5$	$Ba_2InErSe_5$
Ba1−Se4×2	3.2610(9)	3.256(1)	3.261(1)	3.262(1)	3.259(1)	3.259(2)
Ba1−Se1×2	3.270(1)	3.270(1)	3.273(1)	3.272(1)	3.271(2)	3.266(2)
Ba1−Se2×2	3.289(1)	3.293(1)	3.296(1)	3.292(1)	3.290(2)	3.287(2)
Ba1−Se3	3.465(1)	3.539(2)	3.511(2)	3.492(2)	3.459(2)	3.446(2)
Ba1−Se5	3.824(1)	3.849(2)	3.842(2)	3.837(2)	3.815(2)	3.801(2)
Ba2−Se1×2	3.250(1)	3.251(1)	3.254(1)	3.253(1)	3.247(2)	3.244(2)
Ba2−Se2	3.274(1)	3.302(2)	3.299(2)	3.288(2)	3.276(2)	3.267(2)
Ba2−Se4×2	3.317(1)	3.318(1)	3.322(1)	3.321(1)	3.313(1)	3.310(2)
Ba2−Se3×2	3.531(1)	3.490(1)	3.506(2)	3.516(1)	3.521(2)	3.529(2)
Ba2−Se5	3.590(1)	3.536(2)	3.552(2)	3.572(2)	3.578(2)	3.594(2)
In−Se4	2.505(1)	2.506(2)	2.510(2)	2.506(2)	2.507(2)	2.505(2)
In−Se5×2	2.6007(8)	2.610(1)	2.610(1)	2.606(1)	2.603(1)	2.596(1)
In−Se3	2.684(1)	2.690(2)	2.694(2)	2.693(2)	2.682(2)	2.685(2)
Ln−Se1	2.747(1)	2.817(2)	2.793(2)	2.776(2)	2.746(2)	2.732(2)
Ln−Se2×2	2.824(1)	2.885(1)	2.865(1)	2.851(1)	2.825(1)	2.806(1)
Ln−Se3×2	2.933(1)	2.986(1)	2.971(1)	2.955(1)	2.936(1)	2.918(1)
Ln−Se5	3.044(2)	3.100(2)	3.089(2)	3.069(2)	3.045(2)	3.032(2)

Er), and Se in the molar ratio of 4:1:2:3 were heated to 1173 K in 20 h, kept at that temperature for 72 h, and then the furnace was turned off.

X-ray powder diffraction analysis of the resultant powder samples were performed at room temperature in the angular range of 2θ = 10−70° with a scan step width of 0.02° and a fixed counting time of 0.2 s/step using an automated Bruker D8 X-ray diffractometer equipped with a diffracted monochromator set for Cu Kα (λ = 1.5418 Å) radiation. The experimental powder X-ray diffraction patterns were found to be in agreement with the calculated pattern on the basis of the single crystal crystallographic data of Ba_2MLnSe_5 (M = Ga, In; *Ln* = Y, Nd, Sm, Gd, Dy, Er).

Structure Determination. The single crystal X-ray diffraction measurements were performed on a Rigaku AFC10 diffractometer equipped with a graphite-monochromated K_α (λ = 0.71073 Å) radiation at 153 K. The CrystalClear software[41] was used for data extraction and integration, and the program XPREP[42] was used for face-indexed absorption corrections.

The structure was solved with Direct Methods implemented in the program SHELXS and refined with the least-squares program SHELXL of the SHELXTL.PC suite of programs.[42] The program STRUCTURE TIDY[43] was then employed to standardize the atomic coordinates. Additional experimental details are given in Tables 1 and 2, and selected metrical data are given in Tables 3 and 4. Further information may be found in the Supporting Information.

Diffuse Reflectance Spectroscopy. A Cary 1E UV−visible spectrophotometer with a diffuse reflectance accessory was used to

dx.doi.org/10.1021/ic300604a | Inorg. Chem. 2012, 51, 6860−6867

measure the spectra of Ba_2MLnSe_5 (M = Ga, In; *Ln* = Y, Nd, Sm, Gd, Dy, Er) over the range 350 nm (3.54 eV) to 2000 nm (0.62 eV).

Magnetic Susceptibility Measurements. The magnetic susceptibility for powder samples of $Ba_2GaGdSe_5$ and $Ba_2InLnSe_5$ (*Ln* = Nd, Sm, Gd, Dy, Er) were measured by using a Quantum Design SQUID magnetometer (MPMS7T Quantum Design) between 2 and 300 K in an applied field of 10 KOe. The powder samples were put in a sample holder and cooled to the low-temperature limit. After the magnetic field was applied, the samples were slowly warmed to 300 K (zero-field cooling, ZFC), followed by cooling in the field (field cooling, FC). The susceptibility was calculated by dividing by the applied field.

Second-Harmonic Generation Measurement. Optical second-harmonic generation (SHG) tests of $Ba_2InLnSe_5$ (*Ln* = Y, Nd, Sm, Gd, Dy, Er) were performed on the powder samples by means of the Kurtz-Perry method.[44] Fundamental 2090 nm light was generated with a Q-switched Ho:Tm:Cr:YAG laser. The particle sizes of the sieved samples are 80−100 μm. Microcrystalline $AgGaSe_2$ of similar particle size served as reference.

RESULTS AND DISCUSSION

Synthesis. Twelve new selenides Ba_2MLnSe_5 (M = Ga, In; *Ln* = Y, Nd, Sm, Gd, Dy, Er) have been synthesized by traditional high-temperature solid state reactions with the yields of at least 50% based on *Ln*. In view of the high reaction temperature and the ease of forming these compounds, they are probably thermodynamically stable compounds. We also tried to synthesize analogues containing other rare-earth elements available to us, namely, La, Ce, Pr, Tb, Ho, and Yb. On the basis of EDX analysis, the products should also contain compounds with the Ba_2MLnSe_5 stoichiometry. However, the crystals are of poor crystalline quality and are unsuitable for single crystal X-ray diffraction analysis. Several trials have been attempted to improve the crystal quality, but failed. Thus in the paper, we only report the 12 members of which good crystals could be obtained.

Structure. $Ba_2GaLnSe_5$ (*Ln* = Y, Nd, Sm, Gd, Dy, Er). The six Ga-containing compounds $Ba_2GaLnSe_5$ (*Ln* = Y, Nd, Sm, Gd, Dy, Er) are isostructural. They crystallize in a new structure type in the centrosymmetric space group $P\bar{1}$ of the triclinic system. In the asymmetric unit, there are two crystallographically independent Ba atoms, one independent Ga atom, one *Ln* atom, and five Se atoms. All are at general positions with 100% occupancy. Because there are no metal−metal or Se−Se bonds in the structures, the oxidation states of 2+, 3+, 3+, and 2− can be assigned to Ba, Ga, *Ln*, and Se, respectively.

The structure of Ba_2GaYSe_5 is illustrated in Figure 1. The basic structural unit of Ba_2GaYSe_5 is an infinite one-dimensional $^{\infty}_{1}[GaYSe_5]^{4-}$ anionic chain built from YSe_6 octahedra and $GaSe_4$ tetrahedra. The YSe_6 octahedra are connected to each other by edge-sharing to form a chain, and then isolated $GaSe_4$ tetrahedra are attached on both sides of the chain via edge-sharing to produce the infinite one-dimensional $^{\infty}_{1}[GaYSe_5]^{4-}$ anionic chains (Figure 2), which are parallel along the *b*-axis and separated by Ba^{2+} cations in a bicapped trigonal prism coordination environment.

$Ba_2InLnSe_5$ (*Ln* = Y, Nd, Sm, Gd, Dy, Er). The six In-containing isostructural compounds $Ba_2InLnSe_5$ (*Ln* = Y, Nd, Sm, Gd, Dy, Er) belong to the Ba_2BiInS_5 structure type[45] and crystallize in the noncentrosymmetric space group $Cmc2_1$ of the orthorhombic system. The asymmetric unit contains two crystallographically unique Ba atoms, one In atom, one *Ln* atom, and five Se atoms, all at the Wyckoff positions 4*a* with *m* symmetry. Because there are no metal−metal or Se−Se bonds in the structures, the oxidation states of 2+, 3+, 3+, and 2− can be assigned to Ba, In, *Ln*, and Se, respectively.

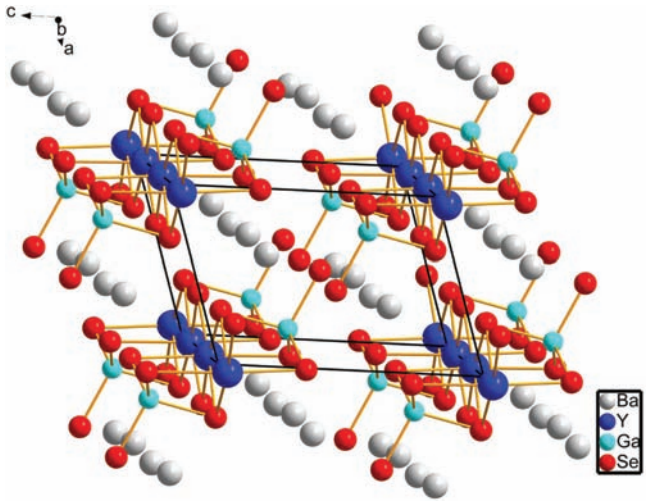

Figure 1. Unit cell of the Ba_2GaYSe_5 structure.

As illustrated in Figure 3, the structure of Ba_2InYSe_5 contains one-dimensional $^{\infty}_{1}[InYSe_5]^{4-}$ anionic chains separated by charge-compensating Ba^{2+} cations, which are surrounded by eight Se atoms in a bicapped trigonal prism geometry. The YSe_6 octahedra themselves form one-dimensional chain by edge-sharing and $InSe_4$ tetrahedra themselves generate another kind of chain via corner-sharing. These two kinds of chains are further interconnected through common Se atoms to generate the $^{\infty}_{1}[InYSe_5]^{4-}$ anionic chains running along *a* direction (Figure 4). Within a single $^{\infty}_{1}[InYSe_5]^{4-}$ anionic chain, the longest Y−Se bonds in the YSe_6 octahedra, the Y−Se5 (3.043 (1) Å) bonds, are almost pointing to the same direction roughly along *b* (Figure 4). However, in the crystal structure, these $^{\infty}_{1}[InYSe_5]^{4-}$ anionic chains can be grouped into pairs within which the direction of longest Y−Se bonds in one chain is roughly opposite to that in the other (Figure 3), which essentially destroys the polar arrangements of the Y−Se bonds on the whole.

Selected bond distances for Ba_2MLnSe_5 (M = Ga, In; *Ln* = Y, Nd, Sm, Gd, Dy, Er) are listed in Tables 3 and 4. The ranges of distances are Ba−Se: 3.218(1)−3.859(2) Å; Ga−Se: 2.346(2)−2.484(1) Å; In−Se: 2.505(1)−2.821(2) Å; Y−Se: 2.747(1)−3.044(2) Å; Nd−Se: 2.817(2)−3.100(2) Å; Sm−Se: 2.793(2)−3.089(2) Å; Gd−Se: 2.776(2)−3.069(2) Å; Dy−Se: 2.746(2)−3.045(2) Å; and Er−Se: 2.732−3.032(2) Å. These values are normal for bicapped trigonal prismatically coordinated Ba, tetrahedrally coordinated M (M = Ga, In), and octahedrally coordinated *Ln* atoms respectively. For example, they are close to those of 3.305(1) to 3.705(1) Å for Ba−Se in $Ba_4AgGa_5Se_{12}$;[46] 2.361(2)−2.488(2) Å for Ga−Se in $BaGa_4Se_7$;[38] 2.513(1) to 2.626(1) Å for In−Se in $Ba_2In_2Se_5$;[47] 2.879(2)−2.910(2) Å for Y−Se in $AgBaYSe_3$;[48] 2.888(1)−3.038(1) Å for Nd−Se in $CsCuNd_2Se_4$;[49] 2.9343(4)−2.9577(3) Å for Sm−Se in $CsSmCdSe_3$;[26] 2.9232(5)−2.9440(4) Å for Gd−Se in $CsGdCdSe_3$;[26] 2.8931(4)−2.9277(3) Å for Dy−Se in $CsDyCdSe_3$;[26] and 2.8464(6)−2.8473(5) Å for Er−Se in $CsErZnSe_3$.[27] According to the lattice constants and the *Ln*-Se bond distances of Ba_2MLnSe_5 (M = Ga, In; *Ln* = Y, Nd, Sm, Gd, Dy, Er), the lanthanide contraction is clearly evident in this series of compounds.

dx.doi.org/10.1021/ic300604a | *Inorg. Chem.* 2012, 51, 6860−6867

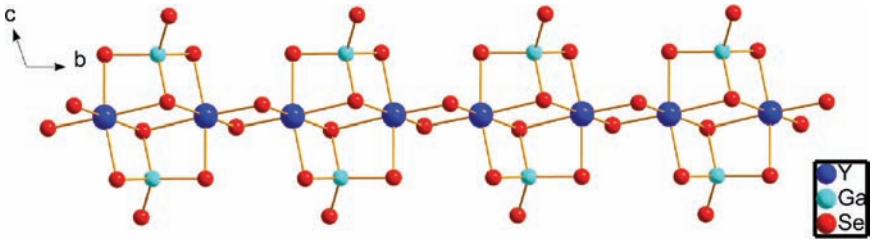

Figure 2. $^{\infty}_{1}[GaYSe_5]^{4-}$ anionic chain in Ba_2GaYSe_5.

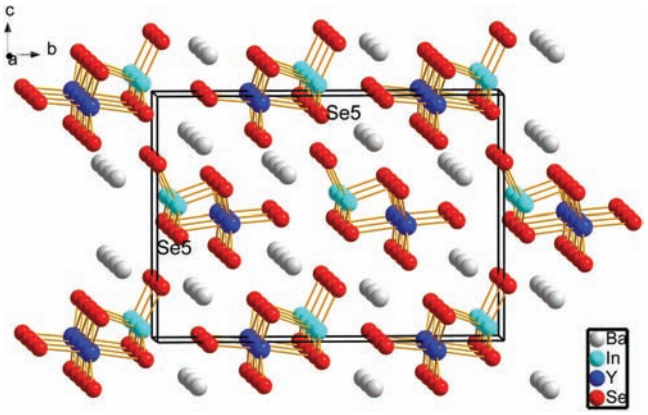

Figure 3. Unit cell of the Ba_2InYSe_5 structure (the Se5 atoms are labeled on a pair of $^{\infty}_{1}[InYSe_5]^{4-}$ anionic chains to indicate the opposite directions of the longest Y–Se5 bonds between the two chains).

Besides, the $LnSe_6$ octahedra in these $Ba_2InLnSe_5$ (Ln = Y, Nd, Sm, Gd, Dy, Er) compounds are less distorted than the BiS_6 octahedra in the isostructural Ba_2BiInS_5 compound: the largest difference in Ln-Se bond lengths within these $LnSe_6$ octahedra is 0.307 (2) Å in $Ba_2InGdSe_5$, while the largest difference in the Bi–S bond lengths within the BiS_6 octahedra is 0.630 (2) Å in Ba_2BiInS_5. Clearly, the stereochemical activity of the $6s^2$ lone pair of Bi leads to the much larger distortion of the BiS_6 octahedra.

The structural difference between the six Ga-containing compounds (space group $P\bar{1}$) and the six In-containing compounds (space group $Cmc2_1$) results from the different connectivity between the MQ_4 tetrahedra and LnQ_6 octahedra. In the Ga-containing compounds, the isolated $GaSe_4$ tetrahedra are alternately located on the two sides of the chain of $LnSe_6$ octahedra and inversion centers can be found between the $GaSe_4$ tetrahedra, while the $InSe_4$ tetrahedra in the In-containing compounds share corners to form a one-dimensional chain on only one side of the chain of $LnSe_6$ octahedra. The different packing modes of the MQ_4 tetrahedra are probably due to the different size of the Ga^{3+} and In^{3+} cations, as the Ga–Se bond length may not be long enough to form a one-dimensional chain which could match the chain of $LnSe_6$ octahedra in view of the interatomic spacing. The effect of cation sizes on the crystal structure have also been shown in other compounds.[50,51] For example, $LiAsS_2$ is noncentrosymmetric, while $NaAsS_2$ is centrosymmetric, and the noncentrosymmetric structure of $Li_{1-x}Na_xAs_2$ holds up to 40% sodium.

Experimental Band Gaps. On the basis of the UV–visible–NIR diffuse reflectance spectra of Ba_2MLnSe_5 (M = Ga, In; Ln = Y, Nd, Sm, Gd, Dy, Er) (Figures 5 and 6), the band gaps can be deduced by the straightforward extrapolation method.[52] As shown in Table 5, the band gaps range from 1.87 (2) eV to 2.34 (2) eV for the six Ga-containing selenides and from 2.20 (2) eV to 2.31 (2) eV for the six In-containing compounds. As shown in Figures 5 and 6, several compounds exhibit broad absorption bands below their respective optical band gaps, which may originate from the typical f-f transitions of Ln^{3+} ions.[53] For example, the observed absorption bands of

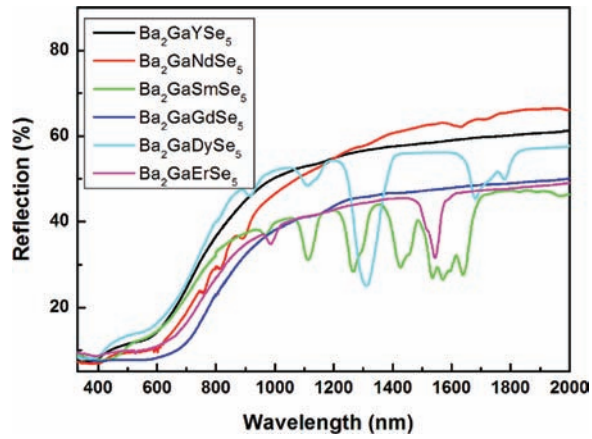

Figure 5. Diffuse reflectance spectra of $Ba_2GaLnSe_5$ (Ln = Y, Nd, Sm, Gd, Dy, Er).

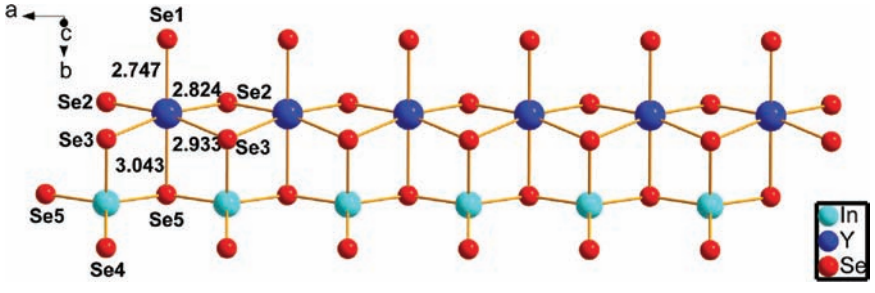

Figure 4. $^{\infty}_{1}[InYSe_5]^{4-}$ anionic chain in Ba_2InYSe_5 with the bond lengths in the YSe_6 octahedra shown (the unit for the bond length is Å).

dx.doi.org/10.1021/ic300604a | Inorg. Chem. 2012, 51, 6860–6867

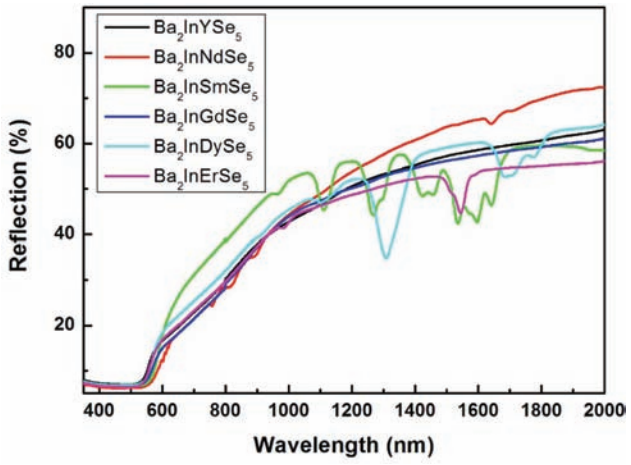

Figure 6. Diffuse reflectance spectra of $Ba_2InLnSe_5$ (*Ln* = Y, Nd, Sm, Gd, Dy, Er).

Table 5. Band Gaps of Ba_2MLnSe_5 (M = Ga, In; *Ln* = Y, Nd, Sm, Gd, Dy, Er)

compound	bandgap (eV)	compound	bandgap (eV)
Ba_2GaYSe_5	2.31 (2)	Ba_2InYSe_5	2.31 (2)
$Ba_2GaNdSe_5$	2.18 (2)	$Ba_2InNdSe_5$	2.20 (2)
$Ba_2GaSmSe_5$	2.27 (2)	$Ba_2InSmSe_5$	2.22 (2)
$Ba_2GaGdSe_5$	1.87 (2)	$Ba_2InGdSe_5$	2.24 (2)
$Ba_2GaDySe_5$	2.35 (2)	$Ba_2InDySe_5$	2.27 (2)
$Ba_2GaErSe_5$	1.95 (2)	$Ba_2InErSe_5$	2.29 (2)

$Ba_2InErSe_5$ at approximately 985 and 1545 nm are due to the transition from the ground state $^4I_{15/2}$ to $^4I_{11/2}$ and $^4I_{13/2}$, respectively.[54] The absorption bands of $Ba_2InDySe_5$ located at approximately 1105 nm, 1305 nm, and 1685−1775 nm may be assigned to transition from the ground state $^6H_{15/2}$ to $^6H_{7/2}$ ($^6F_{9/2}$), $^6H_{9/2}$ ($^6F_{11/2}$), and $^6H_{11/2}$, respectively.[53] It is a bit surprising that the band gaps of yellow Ga-containing compounds are comparable or even a bit smaller than those of red In-containing phases. A tentative explanation may be found in view of the crystallinity: although the XRD patters of the polycrystalline samples did not show any extra peaks for all compounds, the crystallinity of the six Ga-compounds are obviously worse than that of the six In-containing compounds based on the intensity of the XRD peaks; such poor crystallinity may have some influence on the measured band gaps on diffuse reflectance spectra.

Magnetic Susceptibility Measurements. Temperature dependence of the molar magnetic susceptibilities (χ_m) and the inverse magnetic susceptibilities ($1/\chi_m$) for $Ba_2GaGdSe_5$ and $Ba_2InLnSe_5$ (*Ln* = Nd, Sm, Gd, Dy, Er) are shown in the Figure 7. The zero-field-cooled (ZFC) magnetic susceptibility and the field-cooled (FC) magnetic susceptibility data are essentially superimposable at all temperatures. The susceptibility data were fit by a least-squares method to the Curie−Weiss equation $\chi_m = C/(T - \theta)$, where *C* is the Curie constant and θ is the Weiss constant. The effective magnetic moments (μ_{eff} (total)) were calculated from the equation μ_{eff} (total) = $(7.997C)^{1/2}\mu_B$.[55]

As shown in Figure 7, they are paramagnetic and obey the Curie−Weiss law over the entire experimental temperature range except for $Ba_2InSmSe_5$. Table 6 lists the values of C and θ generated by the linear fitting of $1/\chi_m$ with T over the whole temperature, and the calculated effective magnetic moments μ_{eff} for each compound except $Ba_2InSmSe_5$. The calculated effective magnetic moments are close to the theoretical values for Ln^{3+} ion.[56] The negative θ values for the four In-containing rare-earth selenides $Ba_2InLnSe_5$ (*Ln* = Nd, Gd, Dy, Er) may indicate weak short-range antiferromagnetic interaction among the adjacent Ln^{3+} cations, while the small positive θ value for $Ba_2GaGdSe_5$ may indicate rather weak short-range ferromagnetic interaction among the Gd^{3+} cations. The magnetic data for $Ba_2InSmSe_5$ do not follow the Curie−Weiss law because its effective magnetic moment of the 4f electrons has a temperature dependence arising from low-lying multiplets.[57] The distinct magnetic behavior of $Ba_2InSmSe_5$ is typical for Sm^{3+} chalcogenides.[8,26,27]

SHG Measurement. With the use of the 2090 nm laser as fundamental wavelength, the powder SHG properties of the $Ba_2InLnSe_5$ (*Ln* = Y, Nd, Sm, Gd, Dy, Er) compounds were measured. The SHG signal intensity of Ba_2InYSe_5 was close to that of $AgGaSe_2$, which was the largest among the six compounds. The $Ba_2InLnSe_5$ (*Ln* = Gd, Er) compounds have very weak SHG responses while the SHG responses of the Nd-, Sm-, Dy-compounds are undetectable. Obviously, in the $Ba_2InLnSe_5$ (*Ln* = Y, Nd, Sm, Gd, Dy, Er) compounds, the rare-earth metal cation does not affect the crystal structure, but it has an effect on the intensity of the SHG response. Similar phenomena occurred in the series Ln_4GaSbS_9 (*Ln* = Pr, Nd, Sm, Gd−Ho)[22] compounds, and the mechanism for such phenomena is discussed in a very recent paper.[58]

In the earlier study, the isostructural bismuth compound Ba_2InBiS_5 was also reported to exhibit strong NLO responses. On the basis of current research on IR NLO materials, there are basically two kinds of microscopic NLO-active units in inorganic chalcogenides. One kind includes some tetrahedral units especially the MQ_4 (M = Ga, In),[20−22,32−40] and the other kind includes some asymmetric unit centered by a metal cation exhibiting a second-order Jahn−Teller effect.[51,59] From our long time research experience on IR NLO chalcogenides, for the Ba_2InBiS_5 compound, although it was proposed that Bi^{3+} lone pair electrons are essential for the strong (SHG) response, the contribution of $InSe_4$ could not be ignored as there is equal amount of InS_4 and BiS_6.

Actually, as discussed in the crystal structure part, although within a single $^{\infty}_{1}[InBiS_5]^{4-}$ anionic chain, the $6s^2$ lone pair electrons of Bi (or the longest Bi−S bond) are almost pointing to the same direction roughly along *b*; in the crystal structure of Ba_2InBiS_5, these $^{\infty}_{1}[InBiS_5]^{4-}$ anionic chains can be grouped into pairs within which the direction of the $6s^2$ lone pair electrons in one chain is roughly opposite to that in the other chain. Such arrangement is destructive for the generation of large overall NLO response.

In this study, strong NLO response was observed for the yttrium compound Ba_2InYSe_5. Such NLO response may come from the cooperative alignment of $InSe_4$ tetrahedra, or may have some contribution from YSe_6 irregular octahedra although it is less distorted than the BiS_6 in Ba_2InBiS_5. The mechanism of the generation of NLO response in chalcogenides actually needs further investigation, and the more experimental data we have, the more likely we could correctly uncover the underlying mechanism in the future. Thus we believe our research on Ba_2InYSe_5 provides valuable addition to the research on Ba_2InBiS_5

■ CONCLUSIONS

In summary, 12 new rare-earth selenides in the quaternary A/M/*Ln*/Q (A = alkaline-earth; M = group IIIA metal Ga, In; *Ln*

dx.doi.org/10.1021/ic300604a | Inorg. Chem. 2012, 51, 6860−6867

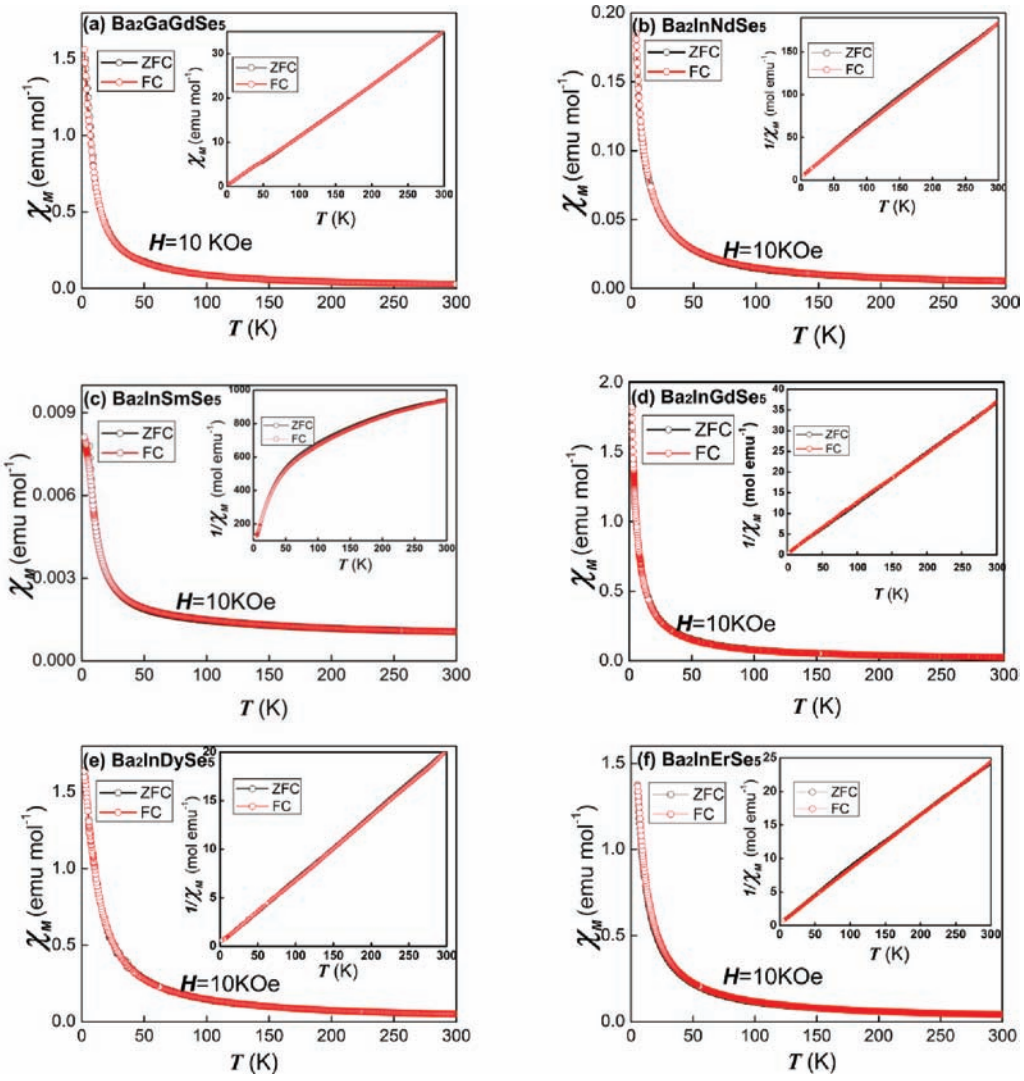

Figure 7. χ_m vs T of $Ba_2GaGdSe_5$ and $Ba_2InLnSe_5$ (Ln = Nd, Sm, Gd, Dy, Er) for FC and ZFC data. Inset shows the plot of $1/\chi_m$ vs T.

Table 6. Magnetic Properties of $Ba_2GaGdSe_5$ and $Ba_2InLnSe_5$ (Ln = Nd, Gd, Dy, Er)

			μ_{eff} (μ_B)	
compound	C (emu K mol^{-1})	θ (K)	obs	theory
$Ba_2GaGdSe_5$	8.62	1.35	8.30	7.94
$Ba_2InNdSe_5$	1.68	−11.16	3.66	3.62
$Ba_2InGdSe_5$	8.23	−2.60	8.11	7.94
$Ba_2InDySe_5$	15.08	−3.60	10.98	10.63
$Ba_2InErSe_5$	12.58	−7.62	10.03	9.59

= rare-earth; Q = S, Se, Te) system, $Ba_2ML nSe_5$ (M = Ga, In; Ln = Y, Nd, Sm, Gd, Dy, Er) were discovered and characterized. The six Ga-compounds $Ba_2GaLnSe_5$ (Ln = Y, Nd, Sm, Gd, Dy, Er) are isostructural and crystallize in a new structure type in the centrosymmetric space group $P\bar{1}$ of the triclinic system. They contain infinite one-dimensional $^{\infty}_{1}[GaLnSe_5]^{4-}$ anionic chains built from $LnSe_6$ octahedral chain and isolated $GaSe_4$ tetrahedra. The isostructural compounds $Ba_2InLnSe_5$ (Ln = Y, Nd, Sm, Gd, Dy, Er) belong to the Ba_2BiInS_5 structure type, crystallize in the non-centrosymmetric space group $Cmc2_1$, and contain infinite one-dimensional $^{\infty}_{1}[InLnSe_5]^{4-}$ anionic chains built from $LnSe_6$ octahedral chains and $InSe_4$ tetrahedral chains. The band gaps of Ba_2MLnSe_5 (M = Ga, In; Ln = Y, Nd, Sm, Gd, Dy, Er), as deduced from their diffuse reflectance spectra, are around 2.2 eV for most compounds. According to magnetic susceptibility measurements, $Ba_2GaGdSe_5$ and $Ba_2InLnSe_5$ (Ln = Nd, Gd, Dy, Er) are paramagnetic, obey the Curie−Weiss law, and have the effective magnetic moments close to the theoretical values, while $Ba_2InSmSe_5$ does not obey the Curie−Weiss law owing to the crystal field splitting. Remarkably, Ba_2InYSe_5 exhibits the strongest powder SHG effects among the In-compounds with intensity close to that of benchmark $AgGaSe_2$, when probed with the 2090 nm laser as fundamental wavelength. Our primary study indicates that Ba_2InYSe_5 may be a candidate for middle-IR NLO materials.

■ ASSOCIATED CONTENT

Supporting Information

Crystallographic file in CIF format for $Ba_2ML nSe_5$ (M = Ga, In; Ln = Y, Nd, Sm, Gd, Dy, Er). This material is available free of charge via the Internet at http://pubs.acs.org.

■ AUTHOR INFORMATION

Corresponding Author

*E-mail: jyao@mail.ipc.ac.cn.

dx.doi.org/10.1021/ic300604a | Inorg. Chem. 2012, 51, 6860−6867

Notes

The authors declare no competing financial interest.

■ ACKNOWLEDGMENTS

This research was supported by the National Basic Research Project of China (No. 2010CB630701), National Natural Science Foundation of China (No. 91122034), and the Ministry of Science and Technology of China (973 Project No. 2011CBA00110).

■ REFERENCES

(1) Beaudry, B. J.; Gschneidner, K. A., Jr. In *Handbook on the Physics and Chemistry of Rare Earths*; Gschneidner, K. A., Jr., Eyring, LeR., Eds.; Elsevier Science Publishers B.V.: New York, 1978.
(2) Cotton, S. *Lanthanides and actinides*; Oxford University Press: New York, 1991.
(3) Sutorik, A. C.; Albritton-Thomas, J.; Kannewurf, C. R.; Kanatzidis, M. G. *J. Am. Chem. Soc.* **1994**, *116*, 7706−7713.
(4) Sutorik, A. C.; Albritton-Thomas, J.; Hogan, T.; Kannewurf, C. R.; Kanatzidis, M. G. *Chem. Mater.* **1996**, *8*, 751−761.
(5) Chan, G. H.; Lee, C.; Dai, D.; Whangbo, M.-H.; Ibers, J. A. *Inorg. Chem.* **2008**, *47*, 1687−1692.
(6) Wakeshima, M.; Furuuchi, F.; Hinatsu, Y. *J. Phys.: Condens. Matter* **2004**, *16*, 5503−5518.
(7) Huang, F. Q.; Mitchell, K.; Ibers, J. A. *Inorg. Chem.* **2001**, *40*, 5123−5126.
(8) Liu, Y.; Chen, L.; Wu, L.-M. *Inorg. Chem.* **2008**, *47*, 855−862.
(9) Bucher, C. K.; Hwu, S.-J. *Inorg. Chem.* **1994**, *33*, 5831−5835.
(10) Patschke, R.; Brazis, P.; Kannewurf, C. R.; Kanatzidis, M. G. *Inorg. Chem.* **1998**, *37*, 6562−6563.
(11) Evenson, C. R., IV; Dorhout, P. K. *Inorg. Chem.* **2001**, *40*, 2409−2414.
(12) Zeng, H.-Y.; Mattausch, H.; Simon, A.; Zheng, F.-K.; Dong, Z.-C.; Guo, G.-C.; Huang, J.-S. *Inorg. Chem.* **2006**, *45*, 7943−7946.
(13) Patschke, R.; Heising, J.; Kanatzidis, M. G. *Chem. Mater.* **1998**, *10*, 695−697.
(14) Zhao, H.-J.; Li, L.-H.; Wu, L.-M.; Chen, L. *Inorg. Chem.* **2009**, *48*, 11518−11524.
(15) Huang, F. Q.; Ibers, J. A. *Inorg. Chem.* **1999**, *38*, 5978−5983.
(16) Aitken, J. A.; Larson, P.; Mahanti, S. D.; Kanatzidis, M. G. *Chem. Mater.* **2001**, *13*, 4714−4721.
(17) Zhao, H.-J.; Li, L.-H.; Wu, L.-M.; Chen, L. *Inorg. Chem.* **2010**, *49*, 5811−5817.
(18) Jin, G. B.; Choi, E. S.; Guertin, R. P.; Booth, C. H.; Albrecht-Schmitt, T. E. *Chem. Mater.* **2011**, *23*, 1306−1314.
(19) Guo, S.-P.; Guo, G.-C.; Wang, M.-S.; Zou, J.-P.; Xu, G.; Wang, G.-J.; Long, X.-F.; Huang, J.-S. *Inorg. Chem.* **2009**, *48*, 7059−7065.
(20) Chen, M.-C.; Li, P.; Zhou, L.-J.; Li, L.-H.; Chen, L. *Inorg. Chem.* **2011**, *50*, 12402−12404.
(21) Zhao, H.-J.; Zhang, Y.-F.; Chen, L. *J. Am. Chem. Soc.* **2012**, *134*, 1993−1995.
(22) Chen, M.-C.; Li, L.-H.; Chen, Y.-B.; Chen, L. *J. Am. Chem. Soc.* **2011**, *133*, 4617−4624.
(23) Carpenter, J. D.; Hwu, S.-J. *Inorg. Chem.* **1995**, *34*, 4647−4651.
(24) Carpenter, J. D.; Hwu, S.-J. *Chem. Mater.* **1992**, *4*, 1368−1372.
(25) Choudhury, A.; Dorhout, P. K. *Inorg. Chem.* **2008**, *47*, 3603−3609.
(26) Mitchell, K.; Huang, F. Q.; McFarland, A. D.; Haynes, C. L.; Somers, R. C.; Van Duyne, R. P.; Ibers, J. A. *Inorg. Chem.* **2003**, *42*, 4109−4116.
(27) Mitchell, K.; Haynes, C. L.; McFarland, A. D.; Van Duyne, R. P.; Ibers, J. A. *Inorg. Chem.* **2002**, *41*, 1199−1204.
(28) Yao, J.; Deng, B.; Sherry, L. J.; McFarland, A. D.; Ellis, D. E.; Van Duyne, R. P.; Ibers, J. A. *Inorg. Chem.* **2004**, *43*, 7735−7740.
(29) Mitchell, K.; Huang, F. Q.; Caspi, E. N.; McFarland, A. D.; Haynes, C. L.; Somers, R. C.; Jorgensen, J. D.; Van Duyne, R. P.; Ibers, J. A. *Inorg. Chem.* **2004**, *43*, 1082−1089.
(30) Chan, G. H.; Sherry, L. J.; Van Duyne, R. P.; Ibers, J. A. *Z. Anorg. Allg. Chem.* **2007**, *633*, 1343−1348.
(31) Meng, C.-Y.; Chen, H.; Wang, P.; Chen, L. *Chem. Mater.* **2011**, *23*, 4910−4919.
(32) Yao, J.; Yin, W.; Feng, K.; Li, X.; Mei, D.; Lu, Q.; Ni, Y.; Zhang, Z.; Hu, Z.; Wu, Y. *J. Cryst. Growth* **2012**, *346*, 1−4.
(33) Badikov, V.; Badikov, D.; Shevyrdyaeva, G.; Tyazhev, A.; Marchev, G.; Panyutin, V.; Petrov, V.; Kwasniewski, A. *Phys. Status Solidi RRL S.* **2011**, *1*, 31−33.
(34) Chemla, D. S.; Kupecek, P. J.; Robertson, D. S.; Smith, R. C. *Opt. Commun.* **1971**, *3*, 29−31.
(35) Boyd, G. D.; Kasper, H. M.; McFee, J. H.; Storz, F. G. *IEEE J. Quantum Electron.* **1972**, *8*, 900−908.
(36) Mei, D.; Yin, W.; Feng, K.; Lin, Z.; Bai, L.; Yao, J.; Wu, Y. *Inorg. Chem.* **2012**, *51*, 1035−1040.
(37) Lin, X.; Zhang, G.; Ye, N. *Cryst. Growth Des.* **2009**, *9*, 1186−1189.
(38) Yao, J.; Mei, D.; Bai, L.; Lin, Z.; Yin, W.; Fu, P.; Wu, Y. *Inorg. Chem.* **2010**, *49*, 9212−9216.
(39) Yin, W.; Feng, K.; He, R.; Mei, D.; Lin, Z.; Yao, J.; Wu, Y. *Dalton Trans.* **2012**, *41*, 5653−5661.
(40) Petrov, V.; Yelisseyev, A.; Isaenko, L.; Lobanov, S.; Titov, A.; Zondy, J.-J. *Appl. Phys. B: Lasers Opt.* **2004**, *78*, 543−546.
(41) *CrystalClear*; Rigaku Corporation: Tokyo, Japan, 2008.
(42) Sheldrick, G. M. *Acta Crystallogr., Sect. A* **2008**, *64*, 112−122.
(43) Gelato, L. M.; Parthé, E. *J. Appl. Crystallogr.* **1987**, *20*, 139−143.
(44) Kurtz, S. K.; Perry, T. T. *J. Appl. Phys.* **1968**, *39*, 3798−3813.
(45) Geng, L.; Cheng, W.-D.; Lin, C.-S.; Zhang, W.-L.; Zhang, H.; He, Z.-Z. *Inorg. Chem.* **2011**, *50*, 5679−5686.
(46) Yin, W.; Feng, K.; Mei, D.; Yao, J.; Fu, P.; Wu, Y. *Dalton Trans.* **2012**, *41*, 2272−2276.
(47) Eisenmann, B.; Hofmann, A. *Z. Anorg. Allg. Chem.* **1990**, *580*, 151−159.
(48) Wu, P.; Christuk, A. E.; Ibers, J. A. *J. Solid State Chem.* **1994**, *110*, 337−344.
(49) Babo, J. M.; Strobel, S.; Schleid, T. *Z. Anorg. Allg. Chem.* **2010**, *636*, 349−355.
(50) Feng, K.; Yin, W.; Yao, J.; Wu, Y. *J. Solid State Chem.* **2011**, *184*, 3353−3356.
(51) Bera, T. K.; Jang, J. I.; Ketterson, J. B.; Kanatzidis, M. G. *J. Am. Chem. Soc.* **2009**, *131*, 75−77.
(52) Schevciw, O.; White, W. B. *Mater. Res. Bull.* **1983**, *18*, 1059−1068.
(53) White, W. B. *Appl. Spectrosc.* **1967**, *21*, 167−171.
(54) Heo, J. *J. Mater. Sci. Lett.* **1995**, *14*, 1014−1016.
(55) O'Connor, C. J. *Prog. Inorg. Chem.* **1982**, *29*, 203−283.
(56) Kittel, C. *Introduction to Solid State Physics*, 6th ed.; Wiley: NewYork, 1986.
(57) Kahn, O. *Molecular Magnetism*; VCH Publishers: New York, 1993.
(58) Zhou, L.-J.; Chen, L.; Li, J.-Q.; Wu, L.-M. *J. Solid State Chem.* **2012**, doi: 10.1016/j. jssc. 2012. 02. 052.
(59) Banerjee, S.; Malliakas, C. D.; Jang, J. I.; Ketterson, J. B.; Kanatzidis, M. G. *J. Am. Chem. Soc.* **2008**, *130*, 12270−12272.